0013-7227/06/$15.00/0
Printed in U.S.A.

Endocrinology 147(8):3652–3661

doi: 10.1210/en.2006-0296

Postnatal Remodeling of Dendritic Structure and Spine Density in Gonadotropin-Releasing Hormone Neurons

Elizabeth C. Cottrell, Rebecca E. Campbell, Seong-Kyu Han, and Allan E. Herbison

Centre for Neuroendocrinology and Department of Physiology, University of Otago School of Medical Sciences, Dunedin 9001, New Zealand

The GnRH neurons represent the output cells of the neuronal network controlling gonadal function. Their activation initiates the onset of puberty, but the underlying mechanisms remain unclear. Using a GnRH-green fluorescent protein mouse model, we have been able to fill individual GnRH neurons with biocytin in the acute brain slice preparation to examine their morphological characteristics across puberty. GnRH neurons in prepubertal male mice [postnatal d 10–15 (PND10–15)] exhibited half as many dendritic and somal spines as adult male mice (>PND60; $P < 0.05$) but, surprisingly, a much more complex dendritic tree with 5-fold greater branch points ($P < 0.05$). Experiments examining somal and proximal dendritic spine numbers *in vivo*, in perfusion-fixed tissue from GnRH-green fluorescent protein mice, revealed the same pattern of approximately twice as many spines on adult GnRH neurons compared with PND10 male mice ($P < 0.01$). In contrast to the spine density alterations, reflecting changing excitatory input, confocal immunofluorescence studies revealed no differences in the numbers of vesicular γ-aminobutyric acid transporter-immunoreactive elements adjacent to GnRH soma or proximal dendrites in prepubertal and adult male mice. Experiments evaluating dendritic tree structure *in vivo* (PND3, -10, and -35 and adult) revealed that GnRH neurons located in the rostral preoptic area, but not the medial septum, exhibited a more complex branching pattern at PND10, but that this was adult-like by PND35. These studies demonstrate unexpected dendritic tree remodeling in the GnRH neurons and provide evidence for an increase in direct excitatory inputs to GnRH neurons across the time of puberty. (*Endocrinology* 147: 3652–3661, 2006)

THE GnRH NEURONS REPRESENT the final output cells of the neuronal network regulating fertility. These neurons are unusual in that they migrate into the brain during embryogenesis (1). Once established in the brain, they exist as a scattered continuum of bipolar- or unipolar-shaped cells that project axons to the median eminence from where they secrete GnRH in a synchronized manner to control pituitary gonadotropin secretion (2). It is now established that the activation of GnRH neurons in late postnatal development initiates the process of puberty; however, the mechanisms underlying the activation of these neurons remain unclear (3–5).

Postnatal neuronal development requires an elaborate interplay between innervating glutamatergic and γ-aminobutyric acid (GABA)ergic axons and dendrites. In the rodent brain, synaptogenesis typically occurs within the first 2–3 postnatal weeks and occurs in a stepwise manner involving a switch from depolarizing to hyperpolarizing $GABA_A$ receptor-mediated transmission associated with *N*-methyl-D-aspartate (NMDA) and then α-amino-3-hydroxy-5-methyl-4-isoxazolepropionic acid (AMPA) receptor-mediated excitation (6, 7). Although intrinsic processes are involved in dendritic morphogenesis, extrinsic inputs to the cell are also critical (8) with the final stabilization of dendritic structure, in particular, being dependent upon developing glutamatergic transmission (9–11). Not surprisingly, GABA and glutamate have received considerable attention with respect to the maturation and activation of the GnRH neurons at puberty. Studies in the female monkey have demonstrated that a decline in inhibitory $GABA_A$ receptor-mediated tone within the vicinity of the GnRH neuron soma is involved in determining the onset of GnRH neuron activation (12, 13). At a cellular level, the subunit composition of the $GABA_A$ receptors expressed by GnRH neurons, their affinity for GABA, and their depolarizing *vs.* hyperpolarizing effect on GnRH neuron excitability are all thought to change across puberty in the mouse (14, 15). Although *in vivo* studies have revealed a clear role for NMDA transmission in regulating puberty onset within the rodent brain (16–19), information on the sites and cellular mechanisms underlying glutamatergic actions are lacking (4, 20).

Using biocytin filling of GnRH neurons *in situ* in GnRH-green fluorescent protein (GFP) transgenic mice, we have recently shown that these cells exhibit very long dendrites as well as numerous somal and dendritic spines (21). As initially established by Gray (22), spines represent the location of excitatory, predominantly glutamatergic, input to neurons (23–25). For example, in the most heavily investigated brain region, the hippocampus, spines are almost exclusively the site of glutamatergic synapses, being devoid of inhibitory or neuropeptidergic inputs (23). Using spine density as an index of excitatory inputs, and vesicular GABA transporter (vGAT) immunofluorescence to assess GABAergic inputs to GnRH neurons (26), we examined whether changes may occur in

First Published Online April 27, 2006

Abbreviations: aCSF, Artificial cerebrospinal fluid; AMPA, α-amino-3-hydroxy-5-methyl-4-isoxazolepropionic acid; FITC, fluorescein isothiocyanate; GABA, γ-aminobutyric acid; GFP, green fluorescent protein; MS, medial septum; NMDA, *N*-methyl-D-aspartate; PF, paraformaldehyde; PND, postnatal day; rPOA, rostral preoptic area; TBS, Tris-buffered saline; vGAT, vesicular GABA transporter.

***Endocrinology* is published monthly by The Endocrine Society (http://www.endo-society.org), the foremost professional society serving the endocrine community.**

direct excitatory and GABAergic inputs to GnRH neurons across postnatal development.

Materials and Methods

Animals

Male homozygous GnRH-EGFP-mut5 mice (C57BL/6J × CBA/Ca) (27) were used for cell-filling experiments, and male wild-type C57BL/6J or homozygous GnRH-GFP male mice (C57BL/6J) (28) were used for immunocytochemical studies. Fluorescent cells located within the rostral preoptic area of GnRH-EGFP-mut5 (27) or the Spergel GnRH-GFP (28) mice have been demonstrated to be GnRH neurons. Male mice in our colonies exhibit reproductive competence at postnatal day 46 (PND46) ± 3 SEM. All mice were housed under 12-h light, 12-h dark cycle conditions with food and water available *ad libitum*. All procedures were approved by the University of Otago Animal Ethics Committee and carried out under Project 66/02.

Biocytin cell-filling experiments

Slice preparation. Prepubertal (PND10–15) and adult (>PND60) GnRH-EGFP-mut5 male mice were killed by cervical dislocation, their brains rapidly dissected out and placed into ice-cold, oxygenated artificial cerebrospinal fluid (aCSF) of the following composition (in mM): 118 NaCl, 3 KCl, 11 d-glucose, 10 HEPES, 25 $NaHCO_3$, 0.5 $CaCl_2$, 6.0 $MgCl_2$ (pH 7.4). Brains were blocked, glued to a chilled vibratome stage, and submerged in chilled oxygenated aCSF, and coronal brain sections (200 μm thick) containing the rostral preoptic area (rPOA) were cut using a Leica VT 1000s vibratome. After cutting, slices were placed in oxygenated recording aCSF composed of (in mM) 118 NaCl, 3 KCl, 11 d-glucose, 10 HEPES, 25 $NaHCO_3$, 2.5 $CaCl_2$, 1.2 $MgCl_2$ (pH 7.4) and left for 1–2 h at 32 C. This period of time has been shown previously to allow for the restabilization of spine numbers after cutting (29, 30). After this, individual brain slices were transferred to the recording chamber of a Zeiss Axioskop fluorescent microscope and held submerged with constant superfusion of oxygenated recording aCSF at 2 ml/min at room temperature.

Cell-filling procedure. Slices were initially examined under fluorescence with a low-power objective to determine the distribution of fluorescent cells. A single, randomly chosen GnRH neuron located in the rPOA was then brought into focus under the high-power objective using fluorescence for 5–10 sec before switching to differential interference contrast optics. Patch pipettes were prepared from thin-walled borosilicate glass capillary tubing (GC150F-10, 1.5 mm outer diameter, 0.86 mm inner diameter; Havard Apparatus Ltd., Edenbridge, UK) on a Sutter P-97 puller and had tip resistances of 5–7 MΩ. The pipette solution contained (in mM) 130 KCl, 5 NaCl, 0.4 $CaCl_2$, 1 $MgCl_2$, 10 HEPES, 1.1 EGTA (pH 7.3), and 0.25% biocytin. After formation of a whole-cell patch using an Axoclamp 2B amplifier to monitor resistance and voltage, the cell was then briefly (5 sec) examined under fluorescence to confirm its fluorescent identity. After achieving whole-cell mode, the pipette was kept attached to the GnRH neuron for 5 min to allow diffusion of biocytin. After detaching the pipette from the cell, slices were maintained in the recording chamber for 30 min and then placed in ice-cold 4% paraformaldehyde (PF) overnight at 4 C. Typically, only one cell was filled in each brain slice. Slices were then transferred to Tris-buffered saline (TBS, pH 7.6) and kept at 4 C until processing for immunocytochemistry.

Imaging and analysis. Slices were rinsed several times and placed in TBS containing Texas Red-avidin-conjugated fluorophore (2.6 μl/ml; Vector Laboratories Inc., Burlingame, CA), 0.3% Triton X-100, and 0.25% BSA for 90 min at room temperature. Sections were then washed thoroughly in TBS, mounted onto gelatin-coated glass slides, coverslipped with Vectashield mountant (Vector), and stored at 4 C.

A total of 13 prepubertal and 25 adult GnRH neurons were successfully filled with biocytin, and these were imaged and analyzed on a Zeiss 510 LSM confocal laser scanning microscope equipped with LSM 510 control software (version 3.2). Cells were imaged using a laser exciting at 543 nm and with a ×63 Plan Apochromat objective (numerical aperture, 1.4) and ×2 zoom function. Stacks of images were collected through the entire neuron, at intervals of 230 nm. After image collection, each neuron was analyzed for 1) cell soma perimeter length (total length of somal membrane at its largest in two dimensions), 2) total number of dendrites projecting from the soma, 3) number of dendritic branch points, defined as the number of points of dendritic bifurcation giving rise to an additional process length of more than 5 μm (31), and 4) somal and dendritic spine density. Spines were identified as protrusions of length less than 5 μm extending from the soma or dendrites, and protrusions of more than 5 μm were classified as filopodia (25). Using the serial collection of 40–70 confocal images for each neuron, spines were counted by scanning through the entire z-series of images and counting spine-like protrusions. Spine numbers were counted along the primary dendrite (defined as the dendritic projection having the greatest diameter on exiting the cell body) and, in the cases of bipolar or multipolar neurons, along the secondary dendrite. The numbers of spines within the initial 50 μm of dendritic length were counted, and subsequent 50-μm lengths were analyzed, separated by 50-μm portions, similar to the analysis employed by Campbell *et al.* (21). Thus, spine numbers were counted at 0–50, 100–150, 200–250 μm, *etc.*, until termination of the dendrite or its loss from the slice. For the typically much shorter secondary dendrite, the total number of spines was counted and divided by the secondary dendrite length to provide results as spines/10 μm. Projections of filled neurons were exported to, and adjustments of brightness and contrast made in, Photoshop (version 7.0; Adobe Systems, San Jose, CA). The cell body size and total number of dendritic projections, branch points, and spine numbers were compared between adult and juvenile filled GnRH neurons. Mean (± SEM) values were obtained for each of the two experimental groups and tested for significance using the nonparametric Mann-Whitney *U* test (GraphPad Software; INSTAT, San Diego, CA). P values < 0.05 were considered to indicate a significant difference.

Assessment of GnRH neuron spine density and GABAergic inputs in vivo

Immunocytochemistry. Four adult (PND60) and four prepubertal (PND10) GnRH-GFP male mice were given an overdose of sodium pentobarbitone solution, perfused transcardially with 10 ml (PND10) or 15 ml (PND60) of a 4% PF solution, decapitated, and their brains were removed. After postfixation in 4% PF for 1 h at room temperature and overnight immersion in 30% sucrose/TBS solution, brains were mounted on a freezing microtome and three sets of 30-μm-thick coronal sections containing the rPOA were cut. Sections were washed thoroughly in TBS and one set incubated in a monoclonal mouse anti-GFP antiserum (Chemicon, Temecula, CA) at 1:5000 in TBS containing 0.3% Triton X-100 and 0.25% BSA for 48 h at 4 C. Sections were then washed three times in TBS before being placed in a fluorescein isothiocyanate (FITC)-conjugated goat antimouse antibody (1:200; TBS with 0.3% Triton X-100, 0.25% BSA) (Alexa Fluor; Molecular Probes/Invitrogen, Eugene, OR) for 2 h at room temperature. A second set of sections was placed in rabbit polyclonal vGAT antibody (1:750; Chemicon) in TBS containing 0.3% Triton X-100, 0.25% BSA, and 2% normal goat serum and incubated at 4 C for 48 h. Sections were rinsed thoroughly in TBS and placed in biotinylated goat antirabbit IgG (1:200; Vector) at room temperature for 2 h. After subsequent washing in TBS, they were then transferred to a streptavidin-conjugated 568-nm fluorophore solution (2.6 μl/ml) (Alexa Fluor; Molecular Probes/Invitrogen) for 2 h again at room temperature. Sections were then washed thoroughly and placed in the monoclonal mouse anti-GFP antisera (Chemicon) at 1:5000 in TBS containing 0.3% Triton X-100 and 0.25% BSA for 48 h at 4 C. This labeling was revealed using a direct FITC-conjugated goat antimouse antibody (1:200; TBS with 0.3% Triton X-100, 0.25% BSA) (Alexa Fluor; Molecular Probes/Invitrogen), and slices were incubated for 2 h at room temperature. All sections were washed thoroughly in TBS, mounted on gelatin-coated glass slides, and coverslipped with Vectashield mounting medium (Vector). Controls for each group included sections in which the primary antibody was omitted from the initial step. The specificity of the Chemicon vGAT antibody has been reported previously (26).

Analysis of spine numbers. Ten labeled neurons located within the rPOA were chosen at random in each age group and were imaged and analyzed using a Zeiss 510 LSM upright confocal laser scanning microscope equipped with LSM 510 control software (version 3.2). An argon laser exciting at 488 nm was used to image the FITC fluorophore. For each cell, a stack of images at 230-nm intervals was collected using a ×63 objective

and a ×2 zoom function through the entire depth of the neuron. Images containing the cell body and initial portion of the primary dendrite were collected. In the absence of biocytin filling, GFP labeling was restricted mostly to less than 50 μm of proximal dendrite. Using the same criteria detailed in the cell-filling experiments, the z-series of slices were scanned and somal and dendritic spine density determined. Because less than 50 μm of proximal dendrite was typically available, the number of spines along the first 10 μm of dendrite were counted for consistency and spine density expressed as number of spines/μm. To enable comparison of these data with that of the biocytin-filled cells, the same method of analysis was applied to the primary dendrite of filled neurons (*i.e.* first 10 μm of dendrite). Spine densities between adults and prepubertal mice were compared using nonparametric Mann-Whitney *U* test.

Analysis of vGAT appositions on GnRH neurons. Fifteen rPOA vGAT/GFP double-labeled cells from each of the four adult and four juvenile animals were selected at random for confocal imaging and subsequent analysis of vGAT inputs. Cells were imaged using an argon laser exciting at 488 nm (GFP) and a helium neon laser exciting at 543 nm (vGAT). All images were taken using a ×63 PlanApochromat objective (numerical aperture, 1.4) and ×2 zoom function. Sections in which the primary vGAT antiserum was omitted were imaged first using the 543-nm laser and the confocal settings adjusted to set background fluorescence at zero. To estimate the density of vGAT appositions, without the need for confocal imaging of the entire neuron, we first established the midpoint of each GnRH neuron by determining the confocal plane in which the nucleus had the greatest diameter. We then collected a z-series stack of seven images for each GnRH neuron consisting of the midpoint and three 230-nm interval images taken from either side. For each image, the numbers of vGAT-labeled puncta directly opposed to GFP-labeled neuronal cell body or primary dendrite were counted and combined to provide mean values for each cell. Typically, the primary dendrite could not be followed for more than approximately 30 μm from the cell body, and therefore, as with the spine analysis, we determined the number of vGAT appositions in the initial 10 μm of dendrite. Data are presented as vGAT appositions/μm of membrane and values from adult and prepubertal GnRH neurons compared with Mann-Whitney *U* test.

Analysis of GnRH neuron dendritic tree structure over postnatal development in vivo

Immunocytochemistry. Four PND3, four PND10, five PND35 and nine adult (>PND60) wild-type male mice were anesthetized and perfusion fixed with 4% PF as detailed above with the exception that PND3 mice received 5 ml 4% PF solution. Three sets of 30-μm coronal sections containing the medial septum (MS) and rPOA were cut from each brain. Endogenous peroxidase activity was quenched by placing sections in a 40% methanol, 1% H_2O_2 TBS solution. Sections were then washed in TBS and placed in a polyclonal rabbit anti-GnRH antibody (LR1 at 1:40,000; R. Benoit, Montreal, Canada), made up in TBS containing 0.3% Triton, 0.25% BSA, and 2% normal goat serum, and incubated at 4 C for 48 h. Sections were then washed in TBS and placed in biotinylated goat antirabbit IgGs (1:200; Vector) for 2 h, washed, and then placed in avidin-biotin complex (ABC kit; Vector) for 2 h at room temperature. Finally, sections were washed and GnRH labeling revealed using the nickel-diaminobenzidine staining method. Sections were washed, mounted on gelatin-coated slides, dried, dehydrated in ethanol and xylene, and coverslipped with DPX mounting medium.

Analysis. Sections were viewed on an Olympus BX-51 microscope at ×10–100 magnification. GnRH-immunoreactive neurons were scored as being either without dendrites (soma only), unipolar, bipolar, or complex in terms of their dendritic structure (see Fig. 5). Complex GnRH neurons were defined as having three or more processes originating from the cell body or any branch point evident on the proximal dendrites. In each mouse, two sections containing GnRH neurons located in the MS and two sections containing GnRH neurons located in the rPOA were selected, and all GnRH neurons in these sections were scored. Values were combined to provide group means (+ SEM) and expressed as a percentage of the total GnRH neuron population analyzed. Statistical analyses were undertaken using ANOVA with *post hoc* Tukey-Kramer tests.

Results

Biocytin cell-filling reveals extensive spine density and dendritic tree remodeling in GnRH neurons across puberty

As noted previously (21), the biocytin filling of GnRH neurons in the acute brain slice enabled the full extent of the GnRH neuron to be visualized including their spines and filopodia (Figs. 1 and 2). In total, 13 prepubertal (PND10–15) and 25 adult (>PND60) biocytin-filled GnRH neurons located in the rPOA were analyzed by confocal microscopy. The GnRH neurons located in this area are responsible for the generation of the GnRH/LH surge that initiates ovulation in rodents (31) including mice (Wintermantle, T. M., R. E. Campbell, K. Porteous, D. Bock, H.-J. Gröne, M. G. Todman, K. S. Korach, E. Greiner, C. A. Pérez, G. Schütz, and A. E. Herbison, submitted). The somal circumference of prepubertal (41 ± 2 μm) and adult (41 ± 1 μm) GnRH neurons was not found to be different (Fig. 3A). No significant differences were detected in the number of dendrites leaving the GnRH soma (prepubertal, 3.0 ± 0.5; adult, 1.9 ± 0.1; $P = 0.08$), but a remarkable divergence in the extent of dendritic branching was observed (Fig. 1, A and B). To evaluate this, we assessed the number of dendritic branch points (32). Prepubertal dendrites exhibited extensive branching with a mean of 5.6 ± 1.0 branch points per cell (range, 1–11) compared with adult GnRH neurons that rarely showed more than one branch point (1.3 ± 0.4 branch points; range, 0–3; $P < 0.01$) (Fig. 3B). Although biased by the observation that the distal extremities of most primary dendrites are cut off when preparing the 200-μm-thick brain slices, the recorded lengths of primary dendrite were not different (prepubertal, 197 ± 24 μm; adult, 232 ± 34 μm).

The analysis of spine numbers also revealed significant differences between adult and prepubertal GnRH neurons. Adult GnRH neurons exhibited twice as many somal spines (24.3 ± 1.8 spines per soma) compared with GnRH neurons of prepubertal mice (12.0 ± 2.2 spines per soma; $P < 0.001$) (Fig. 2). This was also observed in the proximal portion of the primary dendrite (prepubertal, 27.8 ± 5.3 spines per first 50 μm; adult, 40.6 ± 3.1 spines per first 50 μm; $P < 0.05$) but was not observed in the distal dendrite (Fig. 3C). Many GnRH neurons exhibit a bipolar morphology with a much shorter (<50 μm) secondary dendrite originating from the opposite pole of the soma. Analyses of spine numbers on the secondary dendrite revealed the same pattern observed in primary dendrites with numbers of spines/10 μm being 5.5 ± 0.9 in prepubertal GnRH neurons (n = 5) and 9.3 ± 1.4 ($P < 0.05$; n = 10) in adult GnRH neurons. These spine density values were very similar to those of the primary dendrite when recalculated on a spine/10 μm basis (5.4 ± 1.1 spines/10 μm for prepubertal GnRH neurons and 8.1 ± 0.9 spines/10 μm for adult GnRH neurons ($P < 0.05$)). The number of filopodia ranged from 0–3 for each GnRH neuron with no differences detected between prepubertal (0.6 ± 0.2) and adult (0.8 ± 0.2) GnRH neurons.

Spine density differences between prepubertal and adult GnRH neurons also exist in vivo

Previous studies have documented the significant impact of the brain slice procedure upon neuronal spine density (29,

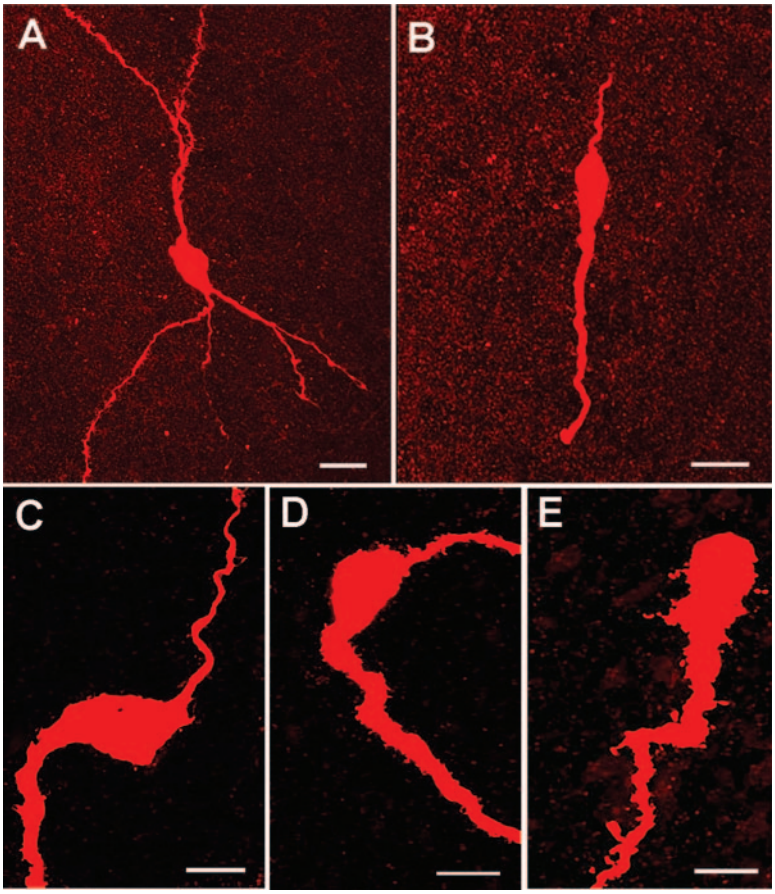

FIG. 1. Prepubertal GnRH neurons exhibit marked morphological differences compared with adult cells. Confocal projection images of biocytin-filled GnRH neurons from prepubertal (A and C) and adult (B, D, and E) GnRH neurons. Note the complex dendritic tree of the PND12 GnRH neuron in A compared with the typically bipolar adult GnRH neuron in B. Note the relative absence of spines on the cell body and proximal dendrite of the PND15 GnRH neuron in C compared with the adult GnRH neurons shown in D and E. *Scale bars*, 10 μm (A and B) and 7.5 μm (C–E).

30). Although we used a brain slice protocol that was optimized for lessening the impact of slicing, we were interested to determine whether our results were a valid approximation of the situation *in vivo*. To do this we employed a GnRH-GFP transgenic mouse line that expresses very high levels of GFP (28) with the idea that GFP might diffuse in a similar manner to biocytin within the cell and enable spine density analyses. Thus, perfusion fixation of GnRH-GFP mice should provide a good indication of spine density *in vivo*. Immunofluorescence for GFP in four adult and four prepubertal GnRH-GFP mice revealed a distribution of cell body staining indistinguishable from that found with GnRH immunoreactivity. Spines were visualized clearly on the GnRH neuron cell soma and the first 30 μm of dendrite. However, beyond the most proximal dendrite, the GFP staining was insufficient to detect spine structures, and accordingly, we limited our analysis to the soma and first 10 μm of dendrite to ensure consistency in our analysis. Confocal analyses revealed that approximately twice as many spines existed on the soma and proximal dendrite of adult GnRH neurons compared with prepubertal GnRH neurons (Fig. 4). At the soma, there was a 2.8-fold increase ($P < 0.001$) in spine numbers from 0.16 $\pm$ 0.02 spines/μm in prepubertal GnRH neurons to 0.45 $\pm$ 0.06 spines/μm in adult GnRH neurons (Fig. 4). Similarly, for the proximal dendrite, we found that spine density increased 1.6-fold ($P < 0.05$) from 0.57 $\pm$ 0.05 spines/μm in prepubertal animals to 0.93 $\pm$ 0.10 spines/μm in adult mice (Fig. 4).

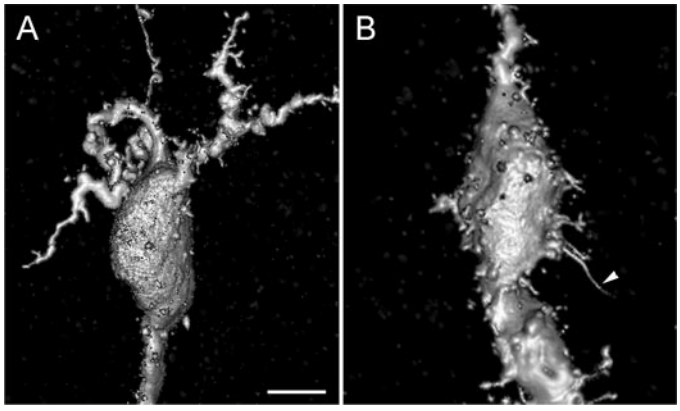

FIG. 2. Three-dimensional rendering of confocal images of biocytin-filled GnRH cell bodies in a prepubertal (A) and adult (B) male mouse. Note the complex dendritic tree and relative absence of spines upon the soma and proximal dendrite of the prepubertal GnRH neuron compared with the adult. *Scale bar*, 5 μm (A and B). *Arrowhead* in B indicates a filopodium.

To evaluate how closely absolute spine density compared in biocytin-filled and perfusion-fixed cells, we recalculated spine density in biocytin-filled cells on the same basis as that done for the perfusion studies. This showed that absolute spine density at the soma was increased in brain slices compared with perfusion-fixed material ($P < 0.05$; Fig. 4). In contrast, spine density at the proximal dendrite was equivalent in both preparations (Fig. 4). Nevertheless, the same developmental increase in spine density at somata and den-

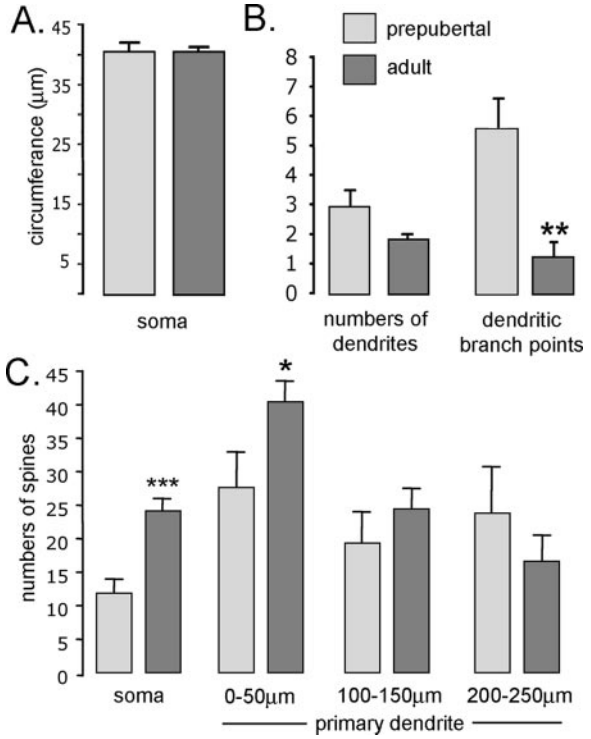

FIG. 3. GnRH neurons in prepubertal mice exhibit increased dendritic branching and spine density. Histograms display somal circumference (A), numbers of dendrites and branch points (B), and spine density of the soma and dendrites (C) of biocytin-filled prepubertal (PND10–15; n = 13) and adult (>PND60; n = 25) GnRH neurons. Note that prepubertal GnRH neurons are highly branched but exhibit a lower spine density on their soma and first 50 μm of primary dendrite compared with adults. *, $P < 0.05$; **, $P < 0.01$; ***, $P < 0.001$.

drites was evident in both cell-filling and perfusion-fixed material (Fig. 4). Together, the results of this study suggested that the spine density analyses performed after biocytin filling *in vitro* provide a good approximation of the situation *in vivo*.

No postnatal developmental differences exist in the number of GABAergic inputs to GnRH neuron soma and proximal dendrites

The changes in spine density revealed above suggest that the numbers of excitatory inputs to the GnRH neurons change across puberty. To evaluate whether changes may also exist in GABAergic inputs to GnRH neurons, we evaluated vGAT appositions to the GnRH soma and proximal dendrite by using confocal analyses. Immunofluorescence for vGAT revealed a heterogeneous pattern of punctate staining (Fig. 5A) similar to that observed previously with this and other vGAT antibodies (26, 33–35). Removal of the primary antibody resulted in an absence of clearly punctate staining. Immunostaining for GnRH neurons with the GFP-specific antibody revealed the typical inverted Y distribution of GnRH soma within the rPOA. Analysis of individual GnRH neurons demonstrated numerous close appositions between vGAT punctae and GnRH neuron somata and proximal dendrites (Fig. 5A). The vGAT punctae were not found on spines.

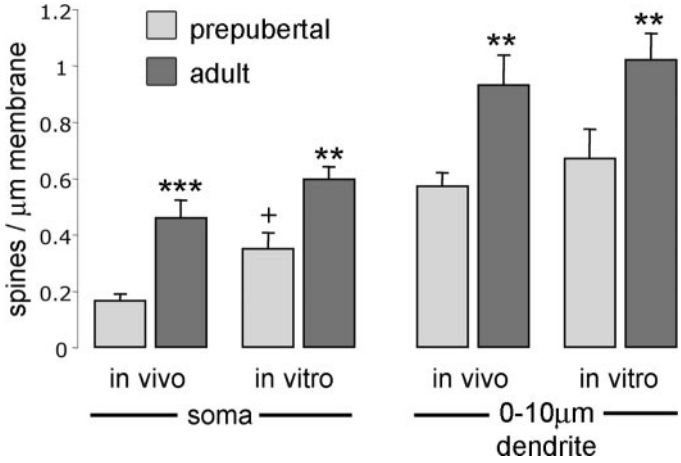

FIG. 4. Comparison of spine density in perfusion-fixed (*in vivo*) and biocytin-filled (*in vitro*) prepubertal (PND10–15) and adult (>PND60) GnRH neurons. Note that all values are given in spines per micrometer. Whereas spine numbers on prepubertal GnRH somata are increased *in vitro* compared with *in vivo* (+, $P < 0.05$), there are no differences in relation to dendritic spine density. In both *in vitro* and *in vivo* circumstances, adult GnRH neurons have significantly greater somal and dendritic spine densities compared with prepubertal GnRH neurons. **, $P < 0.01$; ***, $P < 0.001$.

Quantitative analyses at the level of the confocal images indicated that a higher density of vGAT appositions existed on the proximal dendrites of GnRH neurons compared with their somata (Fig. 5B). However, no differences were detected between prepubertal and adult ages (Fig. 5B).

The dendritic tree of GnRH neurons remodels across postnatal development

The cell-filling studies revealed surprising complexity in the dendritic tree of prepubertal PND10–15 GnRH neurons. To evaluate this further across the GnRH neuronal population as a whole *in vivo* and to gain a better insight into the temporal development of the GnRH neuron dendritic tree, we undertook GnRH immunocytochemical experiments in PND3, PND10, PND35, and adult male wild-type mice. At present, one of the very few ways of defining functional subpopulations of GnRH neurons is on the basis of their anatomical location (2). Immediate-early gene expression patterns in GnRH neurons (31) indicate that the majority of GnRH neurons located in the rPOA are activated to initiate the GnRH surge whereas GnRH neurons in the MS are not (Wintermantle, T. M., submitted). Thus, in this series of studies, we were also interested to determine whether the postnatal dendritic tree remodeling was similar across all GnRH neuron subpopulations.

Immunostaining for GnRH revealed the classic inverted Y distribution of GnRH neuron cell bodies scattered throughout the MS, rPOA, and anterior hypothalamus at all postnatal ages. The mean number of GnRH neuron cell bodies detected per two 30-μm-thick rPOA sections was 37.6 ± 4.0 (PND3), 39.3 ± 3.4 (PND10), 57.4 ± 3.9 (PND35), and 41.4 ± 5.0 (>PND60) with no significant difference detected (ANOVA). We found that GnRH neurons could easily be ascribed a unipolar, bipolar, or complex dendritic morphology (Fig. 6). Whereas dendritic processes could be ascertained for essen-

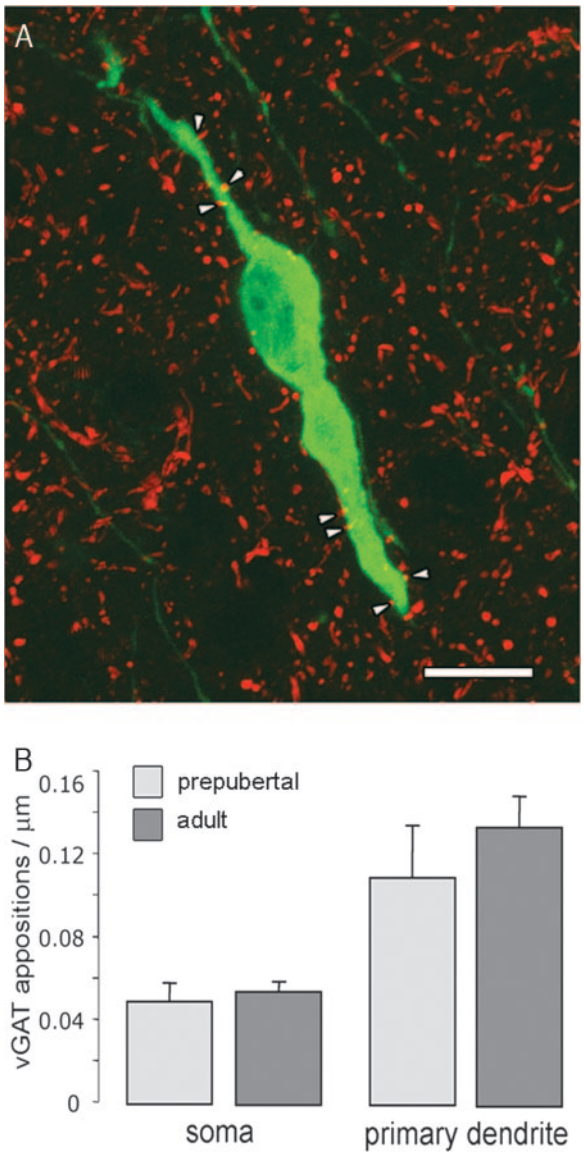

FIG. 5. Numbers of vGAT-immunoreactive punctae adjacent to GnRH neuron soma and the first 10 μm of proximal dendrite are similar in prepubertal (PND10; n = 4) and adult (PND60; n = 4) mice. A, Confocal optical slice (230 nm thick) of a GFP-immunoreactive GnRH neuron (*green*) surrounded by *red* vGAT-immunoreactive elements. Points where the vGAT signal was considered to be immediately adjacent to the GnRH neuron are indicated by *arrowheads*. *Scale bar*, 10 μm.

tially all GnRH neurons in PND10, PND35, and adult mice, most PND3 GnRH neurons appeared as a simple oval immunoreactive soma. At PND3, the breakdown of dendritic morphologies in rPOA GnRH neurons was 52% no dendrite observed, 15% unipolar, 23% bipolar, and 5% complex and was similar for MS GnRH neurons. Because more than 50% of PND3 GnRH neurons could not be ascribed any specific dendritic morphology, statistical comparison with the other age groups was not considered appropriate. At the level of the rPOA, significant developmental changes were detected in the numbers of unipolar and complex GnRH neurons (Fig. 6). The percentage of rPOA GnRH neurons exhibiting complex dendritic morphologies decreased from 41 ± 5% at PND10 to 14 ± 2% and 16 ± 3% in PND35 and adult mice, respectively ($P < 0.001$). Whereas no differences were detected in the percentage of GnRH neurons exhibiting bipolar morphologies (Fig. 5), changes in GnRH neurons with unipolar morphologies were found: PND10, 16 ± 5%; PND35, 31 ± 2%; adult, 33 ± 3% ($P < 0.05$; Fig. 6). In contrast to the rPOA, the percentage of GnRH neurons located in the MS with complex morphologies was not different across postnatal development (PND10, 21 ± 3%; PND35, 9 ± 4%; adult, 13 ± 3%). One significant difference was detected in MS GnRH neurons and represented a shift from unipolar to bipolar dendritic morphology across postnatal development (PND10 unipolar 44 ± 5% *vs.* adult unipolar 30 ± 3%, $P < 0.05$; PND10 bipolar 35 ± 7% *vs.* adult bipolar 56 ± 5%, $P < 0.05$; not shown).

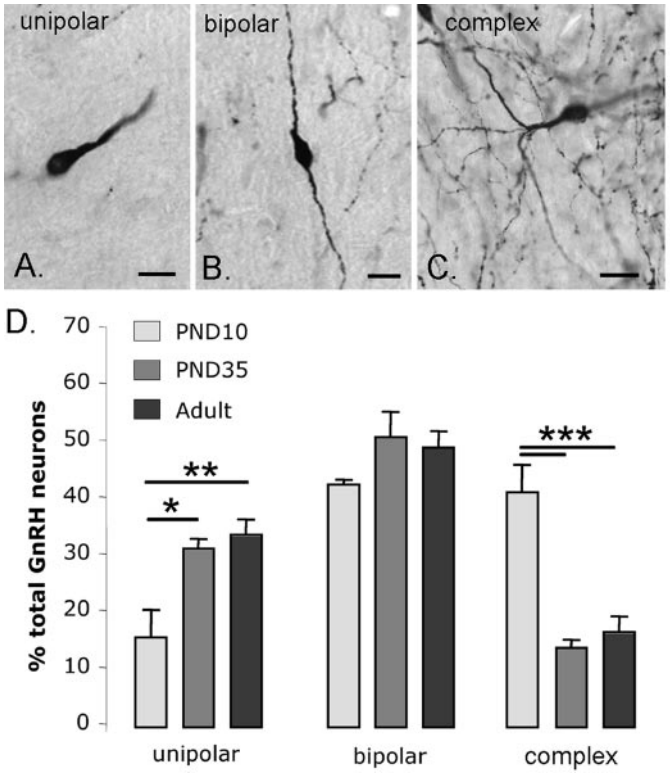

FIG. 6. rPOA GnRH neurons *in vivo* exhibit developmentally regulated changes in dendritic structure. The morphology of individual GnRH-immunoreactive neurons was scored as being unipolar (A), bipolar (B), or complex (C), and then the percentage of rPOA GnRH neurons exhibiting each morphology was determined (D) in PND10 (n = 4), PND35 (n = 5), and adult (n = 9) male mice. Note that the percentage of complex cells decreases whereas that of unipolar neurons increases with age. *, $P < 0.05$; **, $P < 0.01$; ***, $P < 0.001$. *Scale bar*, 10 μm.

Discussion

We show here that the dendritic tree structure and spine density of GnRH neurons changes substantially during postnatal development. Cell-filling experiments demonstrated an approximate doubling in GnRH neuron spine density that was restricted to the soma and proximal dendrites. Subsequent studies with perfusion-fixed material provided evi-

dence that this up-regulation exists *in vivo* and is not an artifact of the brain slice procedure. Whereas these observations indicate that proximal parts of the GnRH neuron receive a substantial increase in excitatory input across puberty, the numbers of GABAergic inputs to these same regions appear stable. Unexpectedly, we found evidence for a major postnatal remodeling of dendritic tree structure in rPOA GnRH neurons. These cells had long been considered to exhibit a relatively simple unipolar or bipolar dendritic morphology in rodents and primates (2, 21). However, both in brain slices and in perfusion-fixed brains, we found that GnRH neurons in the second postnatal week exhibit a highly branched/complex dendritic tree that then becomes much simpler before the activation of these neurons to initiate puberty. Together, these findings reveal an unexpected pattern of dendritic remodeling in these cells and provide evidence for increased excitatory signaling at the level of the GnRH neuron itself across puberty.

Most neuronal networks within the rodent brain exhibit adult-like morphological features by the end of the second or third postnatal week (7, 32, 36–38). Network output cells, such as visual cortex pyramidal cells, exhibit an increase in dendritic spine density from birth through to the end of the third postnatal week (36). We show here that spine density in GnRH neurons increases 2-fold between the end of the second week and adulthood. This result extends the findings of early immunocytochemical studies that reported that the numbers of spiny GnRH neurons increased with postnatal development in the rat (39, 40). Interestingly, we show here that GnRH neurons exhibit the relatively unusual feature of numerous spines on their cell somata. The density of these spines is lower than that observed on the proximal dendrite but, nevertheless, suggests that significant input exists at the cell body in addition to the dendrites.

We found that spine density changes with postnatal development at GnRH somata and proximal dendrites but not at dendritic lengths more than 100 μm from the soma. Because spines represent the location of excitatory inputs to neurons (22, 23, 25), these data indicate that a population of excitatory neurons, targeting specifically the soma and proximal dendrite of the GnRH neuron, increase their synaptic input to GnRH neurons during postnatal development. The identity and location of these neurons is not known, but the topography of changing inputs may have considerable potency given the proximity of the inputs to the axon hillock. Although a recent computational study supports this idea by suggesting that proximal inputs will be more effective in modulating GnRH neuron firing compared with distal dendritic inputs (41), excitatory inputs to distal dendritic regions are not necessarily less effective than proximally placed inputs (42).

The mechanism underlying the developmental change in spine density is not yet established, and in particular, its relationship to fluctuating gonadal steroid concentrations over this period is unknown. Studies undertaken in the hypothalamus and hippocampus have revealed both suppressive and stimulatory effects of estrogen and testosterone upon spine density and synapse formation (43–45). Experiments evaluating the effects of gonadal steroids upon spine density in GnRH neurons are presently underway.

The spine density observations reported here suggest that a significant increase in excitatory input exists directly at the level of the GnRH neurons across puberty. One of the most likely neurotransmitters being used by these inputs is glutamate. Most synapses on spines in the hippocampus are glutamatergic (23), and the increase in spine density from PND10 to adulthood in GnRH neurons correlates well with the increase in expression of the obligatory NMDA receptor NR1 subunit in these cells between PND5 and PND15 (46). The only electrophysiological studies to have examined this issue so far have shown that glutamate receptors develop very late in cultured embryonic GnRH neurons (47) and that cultured PND17–25 GnRH-GFP neurons all respond to glutamate and NMDA (48). Studies *in vivo* have demonstrated that NMDA receptor signaling is important in determining the timing of puberty onset (16–19). As such, it seems reasonable to suggest that an increase in glutamatergic synaptogenesis directly at proximal components of the GnRH neuron may be involved in their maturation and initiation of puberty (Fig. 7).

The other strong contender for a role as a potent excitatory modulator of GnRH neurons in relation to puberty would be kisspeptin. This neuropeptide and its receptor GPR54 are now established to represent an important signaling axis for puberty (49). Whereas essentially all GnRH neurons express transcripts for GPR54 at PND18 and during adulthood in the mouse, the percentage of GnRH neurons displaying electrophysiological responses to kisspeptin increases with postnatal development in mice (50). Thus, the developmental increase in spine numbers may also be associated with the gradual appearance of functional kisspeptin receptors on GnRH neurons. However, it has yet to be determined precisely where kisspeptin inputs synapse on GnRH neurons.

In contrast to spine density, GABA inputs to the GnRH neuron soma and proximal dendrite did not change between PND10 and adulthood. Immunofluorescence detection of vGAT is a reliable marker for GABAergic terminals (33) and has been used successfully for analysis of GABAergic inputs to GnRH neurons in the past (26). Electrophysiological studies have shown that 100% of cultured embryonic GnRH neurons express functional $GABA_A$ receptors as do PND15 and adult GnRH neurons (14, 47). Alongside the present results, these data demonstrate that GnRH neurons are innervated by GABAergic fibers throughout embryonic and postnatal development (Fig. 7). This does not, however, imply that the effects of GABAergic signaling upon GnRH neurons are constant. The profile of $GABA_A$ receptor subunit mRNA expression changes markedly during embryogenesis and between PND20 and adulthood (14, 51), and in addition, $GABA_A$ receptor activation depolarizes embryonic (47) and prepubertal (15, 52) GnRH neurons but likely switches to a hyperpolarizing action after puberty (15, 27; but see Ref. 53) (Fig. 7).

We have identified here an unexpected pattern of dendritic remodeling in GnRH neurons. Previous studies identified rodent and primate GnRH neurons to have a relatively simple dendritic structure with bipolar or unipolar morphologies at all embryonic and postnatal ages (54). We show here that prepubertal, biocytin-filled GnRH neurons exhibit a relatively expansive and branched dendritic tree that then re-

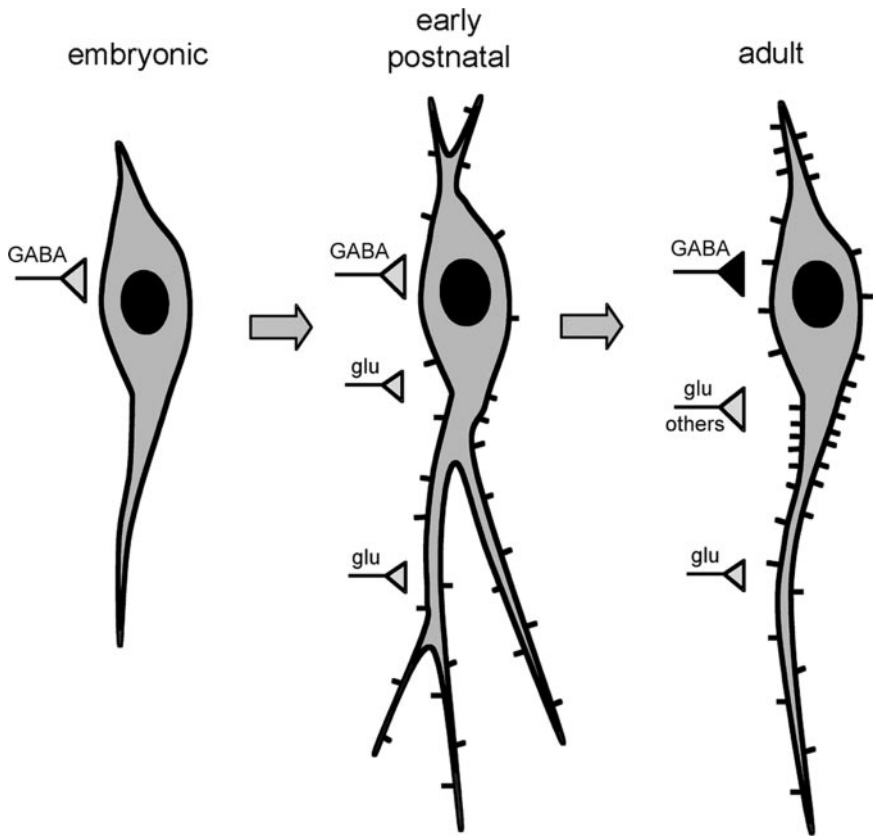

FIG. 7. Schematic diagram depicting possible morphological changes in dendritic tree structure and spine density of GnRH neurons with postnatal development. The relative strength of inputs is indicated by the size of the presynaptic terminal triangle (*gray*, excitatory; *black*, inhibitory). The embryonic GnRH neuron representation is based upon the findings of Kusano and colleagues (47), and GABA data come from Refs. 14 and 15).

models to the characteristic bipolar or unipolar morphology by adulthood (Fig. 7). Experiments evaluating dendritic structure *in vivo* using GnRH immunocytochemistry have supported this finding by showing that GnRH neurons located in the rPOA switch from a complex to unipolar/bipolar dendritic morphology between PND10 and -35. Although the GFP immunocytochemical studies do not enable the morphological characteristics of GnRH neurons to be examined with the same detail attained through biocytin filling, the important advantage of these studies is that whole populations of GnRH neurons located in different brain regions can be imaged. Interestingly, we find little evidence for complex dendritic trees in GnRH neurons residing within the MS at any age. The one functional difference between MS and rPOA GnRH neurons identified so far has been the involvement of specifically rPOA GnRH neurons in the generation of the GnRH surge at proestrus in the mouse (Wintermantle, T. M., submitted). Thus, it is possible that embryonic GnRH neurons destined to control ovulation migrate into the rPOA as simple bipolar/unipolar cells and then, at some time before PND10, extend their dendritic tree before refining it back to a uni-/bipolar morphology before puberty (Fig. 7). Our immunocytochemical studies at PND3 detected most GnRH neurons as oval cell bodies without dendrites. Whether this is a true representation of their morphology or results from a lack of GnRH/GFP peptide in their dendrites is not known and will likely only be resolved after further development of our biocytin-filling technique to enable cells at these young ages to be investigated.

Neurons in other brain areas are known to extend a complex dendritic tree before subsequently refining it to achieve a mature neuronal morphology (32, 55–58). One of the most dramatic examples is in the olfactory cortex where mitral cells extend complex dendritic trees into multiple glomeruli before refining their dendrites to a single glomerulus (57). The molecular mechanisms underlying dendritic remodeling are presently being elucidated and involve cell autonomous intrinsic as well as extrinsic processes (8, 59). Studies in *Xenopus* indicate that two phases of dendritic growth occur, the first being that of the rapid generation of a complex dendritic tree promoted by weak, possibly NMDA-mediated, excitatory inputs followed by a second, slower period of dendrite stabilization mediated by stronger AMPA-dependent synaptic inputs (9, 10). The development of NMDA signaling in GnRH neurons between PND5 and -15 (46), when we observe complex dendritic branching, would fit well with this model. The correlation between increased spine density on stabilized adult dendrites compared with the lower density of spines on the more extensive dendritic tree of prepubertal cells is also compatible.

In summary, we provide here an analysis of direct excitatory and GABA inputs to GnRH neurons across postnatal development. The results suggest that GnRH neurons do indeed receive a substantial increase in excitatory input whereas GABAergic terminal numbers remain constant. Although GABA, glutamate, and kisspeptin have received considerable attention with respect to their role in activating GnRH neurons at puberty, they are not likely to be the sole inputs. Indeed, important roles for other classical neurotransmitters and neuropeptides and glial factors have been

proposed in puberty onset (3–5) (Fig. 7). However, regardless of the specific neurotransmitters involved, an increase in excitatory drive represents a central component of most working models of puberty onset. We provide here evidence that this occurs directly at the GnRH neuron itself.

Acknowledgments

Received March 7, 2006. Accepted April 17, 2006.

Address all correspondence and requests for reprints to: Allan E. Herbison, Centre for Neuroendocrinology, Department of Physiology, University of Otago School of Medical Sciences, P.O. Box 913, Dunedin 9001, New Zealand. E-mail: allan.herbison@stonebow.otago.ac.nz.

This work was supported by the U.K. Wellcome Trust, New Zealand Royal Society Marsden Fund, and a New Zealand Health Research Council Scholarship (ECC).

Author Disclosure Summary: The authors have nothing to declare.

References

1. **Wray S** 2002 Development of gonadotropin-releasing hormone-1 neurons. Front Neuroendocrinol 23:292–316
2. **Herbison AE** 2006 Physiology of the GnRH neuronal network. In: Neill JD, ed. Knobil and Neill's physiology of reproduction. 3rd ed. San Diego: Academic Press; 1415–1482
3. **Terasawa E, Fernandez DL** 2001 Neurobiological mechanisms of the onset of puberty in primates. Endocr Rev 22:111–151
4. **Ojeda SR, Skinner MK** 2006 Puberty in the rat. In: Neill JD, ed. Knobil and Neill's physiology of reproduction. 3rd ed. San Diego: Academic Press; 2061–2126
5. **Plant TM, Witchel SF** 2006 Puberty in nonhuman primates and humans. In: Neill JD, ed. Knobil and Neill's physiology of reproduction. 3rd ed. San Diego: Academic Press; 2177–2230
6. **Ben-Ari Y, Khazipov R, Leinekugel X, Caillard O, Gaiarsa JL** 1997 $GABA_A$, NMDA and AMPA receptors: a developmentally regulated 'menage a trois.' Trends Neurosci 20:523–529
7. **Ben-Ari Y** 2001 Developing networks play a similar melody. Trends Neurosci 24:353–360
8. **Wong RO, Ghosh** 2002 Activity-dependent regulation of dendritic growth and patterning. Nat Rev Neurosci 3:803–812
9. **Wu GY, Zou DJ, Rajan I, Cline H** 1999 Dendritic dynamics in vivo change during neuronal maturation. J Neurosci 19:4472–4483
10. **Rajan I, Cline HT** 1998 Glutamate receptor activity is required for normal development of tectal cell dendrites in vivo. J Neurosci 18:7836–7846
11. **Lee LJ, Lo FS, Erzurumlu RS** 2005 NMDA receptor-dependent regulation of axonal and dendritic branching. J Neurosci 25:2304–2311
12. **Keen KL, Burich AJ, Mitsushima D, Kasuya E, Terasawa E** 1999 Effects of pulsatile infusion of the $GABA_A$ receptor blocker bicuculline on the onset of puberty in female rhesus monkeys. Endocrinology 140:5257–5266
13. **Mitsushima D, Hei DL, Terasawa E** 1994 γ-Aminobutyric acid is an inhibitory neurotransmitter-restricting the release of luteinizing hormone-releasing hormone before the onset of puberty. Proc Natl Acad Sci USA 91:395–399
14. **Sim JA, Skynner MJ, Pape JR, Herbison AE** 2000 Late postnatal reorganization of $GABA_A$ receptor signalling in native GnRH neurons. Eur J Neurosci 12:3497–3504
15. **Han SK, Abraham IM, Herbison AE** 2002 Effect of GABA on GnRH neurons switches from depolarization to hyperpolarization at puberty in the female mouse. Endocrinology 143:1459–1466
16. **MacDonald MC, Wilkinson M** 1990 Peripubertal treatment with *N*-methyl-D-aspartic acid or neonatally with monosodium glutamate accelerates sexual maturation in female rats, an effect reversed by MK-801. Neuroendocrinology 52:143–149
17. **Urbanski HF, Ojeda SR** 1990 A role for *N*-methyl-D-aspartate (NMDA) receptors in the control of LH secretion and initiation of female puberty. Endocrinology 126:1774–1776
18. **Bourguignon JP, Gerard A, Mathieu J, Mathieu A, Franchimont P** 1990 Maturation of the hypothalamic control of pulsatile gonadotropin-releasing hormone secretion at onset of puberty. I. Increased activation of *N*-methyl-D-aspartate receptors. Endocrinology 127:873–881
19. **Brann DW** 1995 Glutamate: a major excitatory transmitter in neuroendocrine regulation. Neuroendocrinology 61:213–225
20. **Clarkson J, Herbison AE,** Development of GABA and glutamate signaling at the GnRH neuron in relation to puberty. Mol Cell Endocrinol, in press
21. **Campbell RE, Han SK, Herbison AE** 2005 Biocytin filling of adult gonadotropin-releasing hormone neurons in situ reveals extensive, spiny, dendritic processes. Endocrinology 146:1163–1169
22. **Gray EG** 1959 Axo-somatic and axo-dendritic synapses of the cerebral cortex: an electron microscope study. J Anat 93:420–433
23. **Sorra KE, Harris KM** 2000 Overview on the structure, composition, function, development, and plasticity of hippocampal dendritic spines. Hippocampus 10:501–511
24. **Shepherd GM** 1996 The dendritic spine: a multifunctional integrative unit. J Neurophysiol 75:2197–2210
25. **Fiala JC, Spacek J, Harris KM** 2002 Dendritic spine pathology: cause or consequence of neurological disorders? Brain Res Brain Res Rev 39:29–54
26. **Ottem EN, Godwin JG, Krishnan S, Petersen SL** 2004 Dual-phenotype GABA/glutamate neurons in adult preoptic area: sexual dimorphism and function. J Neurosci 24:8097–8105
27. **Han SK, Todman MG, Herbison AE** 2004 Endogenous GABA release inhibits the firing of adult gonadotropin-releasing hormone neurons. Endocrinology 145:495–499
28. **Spergel DJ, Kruth U, Hanley DF, Sprengel R, Seeburg PH** 1999 GABA- and glutamate-activated channels in green fluorescent protein-tagged gonadotropin-releasing hormone neurons in transgenic mice. J Neurosci 19:2037–2050
29. **Kirov SA, Petrak LJ, Fiala JC, Harris KM** 2004 Dendritic spines disappear with chilling but proliferate excessively upon rewarming of mature hippocampus. Neuroscience 127:69–80
30. **Kirov SA, Sorra KE, Harris KM** 1999 Slices have more synapses than perfusion-fixed hippocampus from both young and mature rats. J Neurosci 19:2876–2886
31. **Hoffman GE, Smith MS, Verbalis JG** 1993 c-Fos and related immediate early gene products as markers of activity in neuroendocrine systems. Front Neuroendocrinol 14:173–213
32. **Ramoa AS, Campbell G, Shatz CJ** 1988 Dendritic growth and remodeling of cat retinal ganglion cells during fetal and postnatal development. J Neurosci 8:4239–4261
33. **McIntire SL, Reimer RJ, Schuske K, Edwards RH, Jorgensen EM** 1997 Identification and characterization of the vesicular GABA transporter. Nature 389:870–876
34. **Chaudhry FA, Reimer RJ, Bellocchio EE, Danbolt NC, Osen KK, Edwards RH, Storm-Mathisen J** 1998 The vesicular GABA transporter, VGAT, localizes to synaptic vesicles in sets of glycinergic as well as GABAergic neurons. J Neurosci 18:9733–9750
35. **Minelli A, Alonso-Nanclares L, Edwards RH, DeFelipe J, Conti F** 2003 Postnatal development of the vesicular GABA transporter in rat cerebral cortex. Neuroscience 117:337–346
36. **Miller M** 1981 Maturation of rat visual cortex. I. A quantitative study of Golgi-impregnated pyramidal neurons. J Neurocytol 10:859–878
37. **Gomez-Di Cesare CM, Smith KL, Rice FL, Swann JW** 1997 Axonal remodeling during postnatal maturation of CA3 hippocampal pyramidal neurons. J Comp Neurol 384:165–180
38. **Zhu JJ** 2000 Maturation of layer 5 neocortical pyramidal neurons: amplifying salient layer 1 and layer 4 inputs by Ca^{2+} action potentials in adult rat tuft dendrites. J Physiol 526:571–587
39. **Wray S, Hoffman G** 1986 Postnatal morphological changes in rat LHRH neurons correlated with sexual maturation. Neuroendocrinology 43:93–97
40. **Wray S, Hoffman G** 1986 A developmental study of the quantitative distribution of LHRH neurons within the central nervous system of postnatal male and female rats. J Comp Neurol 252:522–531
41. **Roberts CB, Best JA, Suter KJ** 2006 Dendritic processing of excitatory synaptic input in hypothalamic gonadotropin releasing-hormone neurons. Endocrinology 147:1545–1555
42. **Williams SR, Stuart GJ** 2003 Role of dendritic synapse location in the control of action potential output. Trends Neurosci 26:147–154
43. **Flanagan-Cato LM** 2000 Estrogen-induced remodeling of hypothalamic neural circuitry. Front Neuroendocrinol 21:309–329
44. **Cooke BM, Woolley CS** 2005 Gonadal hormone modulation of dendrites in the mammalian CNS. J Neurobiol 64:34–46
45. **Leranth C, Petnehazy O, MacLusky NJ** 2003 Gonadal hormones affect spine synaptic density in the CA1 hippocampal subfield of male rats. J Neurosci 23:1588–1592
46. **Simonian SX, Herbison AE** 2001 Differing, spatially restricted roles of ionotropic glutamate receptors in regulating the migration of GnRH neurons during embryogenesis. J Neurosci 21:934–943
47. **Kusano K, Fueshko S, Gainer H, Wray S** 1995 Electrical and synaptic properties of embryonic luteinizing hormone-releasing hormone neurons in explant cultures. Proc Nat Acad Sci USA 92:918–3922
48. **Kuehl-Kovarik MC, Pouliot WA, Halterman GL, Handa RJ, Dudek FE, Partin KM** 2002 Episodic bursting activity and response to excitatory amino acids in acutely dissociated gonadotropin-releasing hormone neurons genetically targeted with green fluorescent protein. J Neurosci 22:2313–2322
49. **Seminara SB, Kaiser UB** 2005 New gatekeepers of reproduction: GPR54 and its cognate ligand, KiSS-1. Endocrinology 146:1686–1688
50. **Han SK, Gottsch ML, Lee KJ, Popa SM, Smith JT, Jakawich SK, Clifton DK, Steiner RA, Herbison AE** 2005 Activation of gonadotropin-releasing hormone (GnRH) neurons by kisspeptin as a neuroendocrine switch for the onset of puberty. J Neurosci 25:11349–11356
51. **Temple JL, Wray S** 2005 Developmental changes in GABA receptor subunit

composition within the gonadotrophin-releasing hormone-1 neuronal system. J Neuroendocrinol 17:591–599
52. **DeFazio RA, Heger S, Ojeda SR, Moenter SM** 2002 Activation of A-type γ-aminobutyric acid receptors excites gonadotropin-releasing hormone neurons. Mol Endocrinol 16:2872–2891
53. **Moenter SM, DeFazio RA** 2005 Endogenous γ-aminobutyric acid can excite gonadotropin-releasing hormone neurons. Endocrinology 146:5374–5379
54. **Silverman A, Livne I, Witkin JW** 1994 The gonadotrophin-releasing hormone (GnRH), neuronal systems: immunocytochemistry and in situ hybridization. In: Knobil E, Neill JD, eds. The physiology of reproduction. 2nd ed. New York: Raven Press; 1683–1706
55. **Greenough WT, Chang FL** 1988 Dendritic pattern formation involves both oriented regression and oriented growth in the barrels of mouse somatosensory cortex. Brain Res 471:148–152
56. **Marin EC, Watts RJ, Tanaka NK, Ito K, Luo L** 2005 Developmentally programmed remodeling of the *Drosophila* olfactory circuit. Development 132: 725–737
57. **Malun D, Brunjes PC** 1996 Development of olfactory glomeruli: temporal and spatial interactions between olfactory receptor axons and mitral cells in opossums and rats. J Comp Neurol 368:1–16
58. **Dailey ME, Smith SJ** 1996 The dynamics of dendritic structure in developing hippocampal slices. J Neurosci 16:2983–2994
59. **Ye B, Jan YN** 2005 The cadherin superfamily and dendrite development. Trends Cell Biol 15:64–67

***Endocrinology* is published monthly by The Endocrine Society (http://www.endo-society.org), the foremost professional society serving the endocrine community.**